

HOT ROLLING STRATEGIES TO MODULATE Nb INTERACTION WITH MICROSTRUCTURE IN FLAT PRODUCTS*

Beatriz Pereda¹
Pello Uranga²
Beatriz Lopez³
Marcelo Rebellato⁴
J.M. Rodriguez-Ibabe⁵

Abstract

The classical application of Nb microalloying in the development of thermomechanical processes for flat products has been related to its suitability to enhance strain-induced precipitation and get a pancaked austenite prior to transformation. As new steel grades or new lay-outs are being developed, more complex metallurgical conditions need to be evaluated. In this context, Nb microalloying, alone or combined with other microadditions, needs to intervene in a more controlled way in additional steps of the thermomechanical process, besides its conventional strain-induced precipitation role. For example, the hardenability enhancement associated with Nb to properly achieve lower temperature transformation products, demands a proper balance of the Nb amount precipitated during rolling and the one remaining in solid solution. Similar effects are also sought when the final available Nb is used to increase strength through precipitation hardening. This manuscript evaluates how changes in the rolling strategies affect the interaction between Nb(C,N) precipitation and austenite recrystallization at different steps of the rolling process. As the possible interactions between parameters intervening simultaneously are quite complex, the application of microstructural models helps to properly define the best austenite conditioning combined with the convenient amount of Nb in solution, as a function of the final property requirements. Along the manuscript, several strategies will be discussed for the case of hot rolling of flat products comparing both normal and coarse initial austenite grain sizes.

Keywords: Nb microalloying; Thermomechanical processing; Pancaked austenite; Intragranular nucleation.

- ¹ *Dr.-Eng., Researcher, Materials and Manufacturing Division, Ceit and University of Navarra, San Sebastian, Basque Country, Spain.*
- ² *Dr.-Eng., Principal Researcher, Materials and Manufacturing Division, Ceit and University of Navarra, San Sebastian, Basque Country, Spain.*
- ³ *Dr.-Eng., Senior Researcher, Materials and Manufacturing Division, Ceit and University of Navarra, San Sebastian, Basque Country, Spain.*
- ⁴ *Engineer in Metallurgy, RMS, São Paulo, Brasil.*
- ⁵ *Dr.-Eng., President, Senior Researcher, Materials and Manufacturing Division, Ceit and University of Navarra, San Sebastian, Basque Country, Spain.*

1 INTRODUCTION

Thin slab direct rolling (TSDR) is a technology characterized by a continuous evolution, including both the production of new steel grades following this route and the launching of new lay-outs [1, 2]. In this changing context, the role of some traditional microalloying elements can spread from their classical function to new metallurgical rules.

For example, the classical application of Nb in thermomechanical processes is related to its suitability to enhance strain-induced precipitation and get a pancaked austenite prior to transformation. When this approach is implemented in TSDR technologies, the first objective is the refinement of the as-cast microstructure during initial rolling passes by suitable recrystallization steps. This must be achieved prior to any Nb(C,N) strain induced precipitation [3]. This implies the design of a convenient rolling strategy to properly balance the complex recrystallization-precipitation interactions. Based on that, high reductions in initial passes, applied at relatively high temperatures, are some of the most standard options to enhance static recrystallization before any precipitation.

Some authors have suggested that dynamic recrystallization could be a key factor in the refinement of the as-cast grains. In “typical” TSDR rolling strategies, the activation of dynamic recrystallization in coarse as-cast austenite grains requires the application of high strain levels that usually are not easily achieved before Nb precipitation occurrence [4]. Nevertheless, new TSDR lay-outs, in some cases associated with higher and in others with lower initial rolling temperatures than usually applied in thin slab, open the convenience to reanalyze these aspects. In this context, this manuscript evaluates the role of different process parameters that could enhance recrystallization occurrence (both static and dynamic) in conditions corresponding to Nb

microalloyed grades. The analysis will be done considering “normal” initial austenite grain sizes, as those usually present in cold or hot charging, and very coarse austenite grains, as those corresponding to direct charging (as-cast microstructures).

2 MATERIAL AND METHODS

The composition of the steels selected in the study are detailed in Table 1. Both steels correspond to low carbon Nb microalloyed grades with some differences in other elements.

Table 1. Chemical compositions of steels (wt.%)

Steel	C	Mn	Si	Nb	N
A	0.06	1.00	0.35	0.056	0.0100
B	0.05	1.56	0.05	0.060	0.0050

Laboratory multipass torsion tests were performed following the schedule of Figure 1. In order to consider different scenarios, the following conditions were evaluated:

- Coarse initial austenite grain size (direct charging simulation) by reheating at 1420°C.
- Normal initial austenite grain size distribution (reheating at 1250°C to put all Nb into solution).
- Three deformation temperature schedules, as indicated in Table 2. In each case, prior to the first deformation application, a temperature equalizing step was included. Six strain passes were applied, with a total reduction that could correspond to a final sheet thickness of 8-9 mm, considering an initial 60-65 mm thin slab.

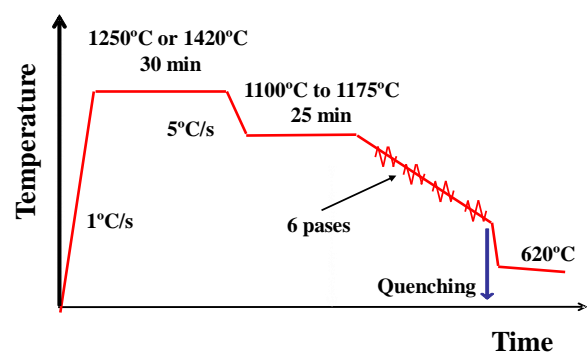


Figure 1. Scheme of the multipass tests performed.

The tests were duplicated for each condition. One of the samples was immediately quenched after the deformation sequence to analyze the austenite microstructure, while in the second case, a coiling simulation step at 620°C was applied and the resulting room temperature microstructure evaluated.

Table 2. Parameters of multipass tests

Pass	Temp (°C)			Strain strain	rate (s ⁻¹)	t _{tip} (s)
	1100*	1150*	1175*	-	-	-
1	1040	1115	1150	0.5	2	5
2	970	1045	1080	0.5	2	5
3	900	975	1010	0.5	2	5
4	850	925	960	0.3	5	3
5	830	905	940	0.3	5	3
6	820	895	930	0.3	5	5
	800**	875**	910**	-	-	-

* It corresponds to the temperature equalizing step.

** Quenching from this temperature.

The evaluation of Nb precipitation was done by TEM analysis in samples quenched after the last deformation pass (replica) and in room temperature microstructures (replica and foils).

The analysis of the softening/hardening mechanisms, affecting austenite evolution during the deformation schedule, was done with the help of MicroSim[®] software (DSP, Direct Strip Processing, v9) [5].

3 RESULTS

3.1 Reheating conditions at 1250°C

At 1250°C, the resulting mean austenite grain size is 210 μm with all Nb in solution. It can be considered a situation close to that corresponding to cold charging.

Figure 2 shows the austenite microstructure obtained with steel A after the application of the schedule with the first strain at T₁=1040°C. It is possible to observe details that suggest the presence of some elongated non-recrystallized grains combined with very fine austenite grains.

The austenite microstructure obtained after the schedule with T₁=1115°C is illustrated in Figure 3. The pancaked nature of the microstructure is more evident and the fraction of small equiaxed grains significantly smaller than that observed in Figure 2.

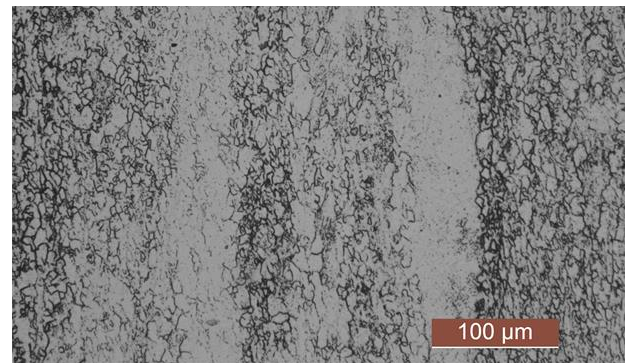
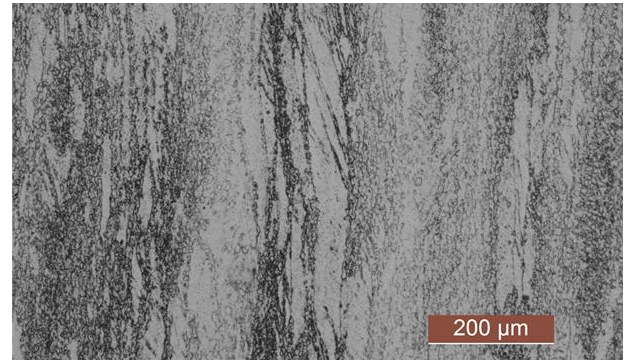
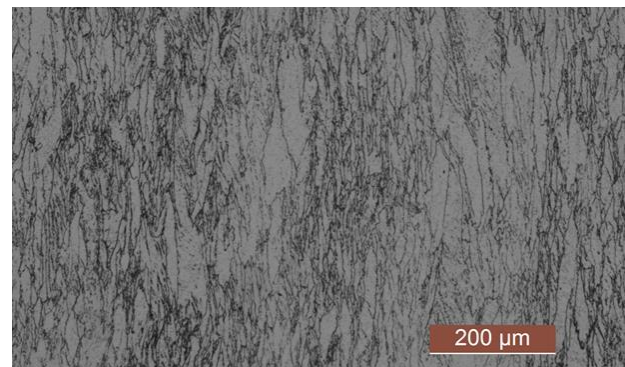


Figure 2. Austenite microstructure after quenching (1250°C-1040°C condition).



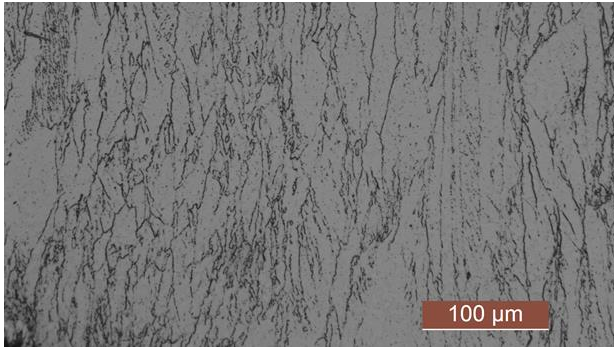


Figure 3. Austenite microstructure after quenching (1250°C-1115°C condition).

The room temperature microstructures of both conditions after coiling simulation are illustrated in Figure 4 and Figure 5.

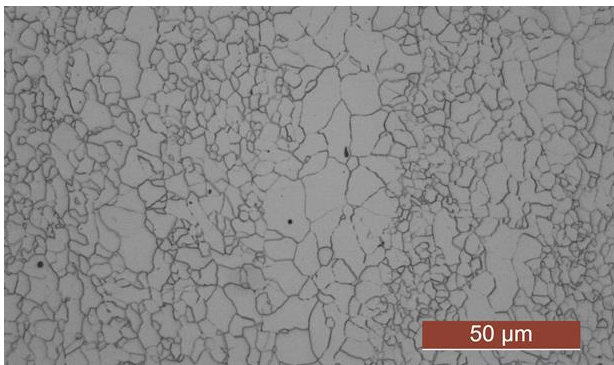
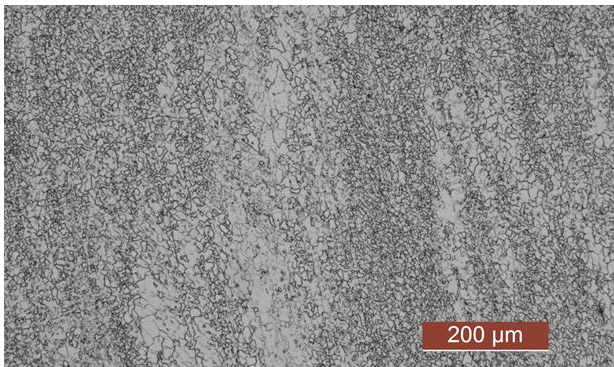


Figure 4. Room temperature microstructure (1250°C-1040°C condition).

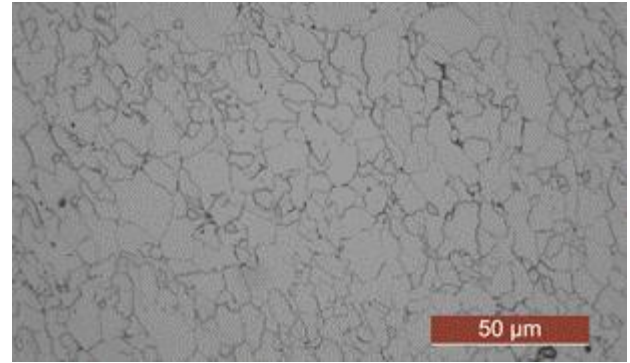
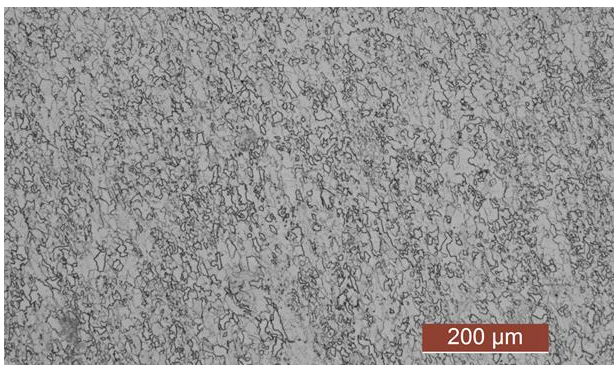


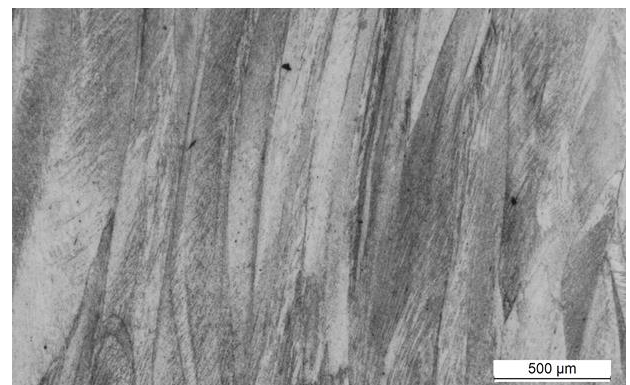
Figure 5. Room temperature microstructure (1250°C-1115°C condition).

They are mainly ferritic with some degree of heterogeneity, more clearly observed in the lower magnification micrograph of Figure 4.

3.2 Reheating conditions at 1420°C

After reheating at 1420°C, the austenite microstructure is composed by coarse grains with a mean value of ~600 μm and some grains as big as 2 mm, closer to a situation representative of direct charging [6]. These conditions were evaluated with steel B.

Figure 6 corresponds to the austenite microstructure after quenching in the condition of $T_1 = 1040^\circ\text{C}$. A very elongated non-recrystallized microstructure can be identified. At higher magnifications, grain boundary serrations and internal microbands are observed. There are not evidences of presence of equiaxed recrystallized grains (in the quenched condition).



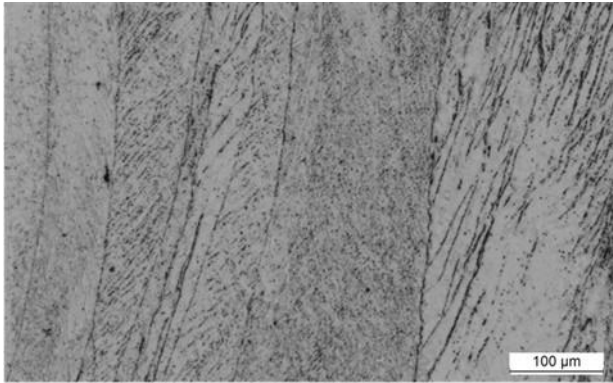


Figure 6. Austenite microstructure after quenching (1420°C-1040°C condition).

The condition corresponding to $T_1 = 1150^\circ\text{C}$ is illustrated in Figure 7. In this case, in addition to the pancaked austenite, it is possible to identify small equiaxed grains. These small grains are quite heterogeneously distributed, as observed in the examples of Figure 8. Finally, there are more evidences of serrations in grain boundaries than those appreciated in Figure 6.



Figure 7. Austenite microstructure after quenching (1420°C-1150°C condition).

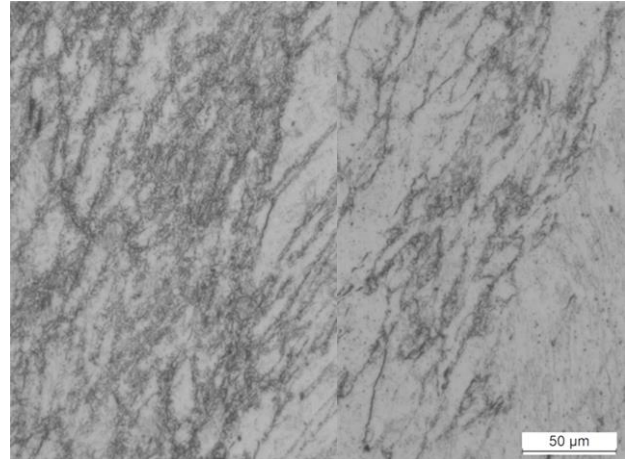


Figure 8. Differences in presence of recrystallized grains (1420°C-1150°C condition).

The microstructures after coiling simulation are shown in Figure 9 and Figure 10. In both situations, in addition to small ferrite grains, there are evidences of heterogeneous areas constituted by coarse grains. While in the condition of $T_1 = 1040^\circ\text{C}$, the heterogeneous fraction is close to 30%, this fraction increases to 50% when the testing condition corresponds to $T_1 = 1150^\circ\text{C}$. In both cases, the mean ferrite grain size measured in the homogeneous areas is very fine and in the range of $3.5 \mu\text{m}$. In the heterogeneous regions with coarse ferrite grains, it is possible to identify also small pearlite colonies. In some cases, these ferritic grains have non-polygonal aspect.



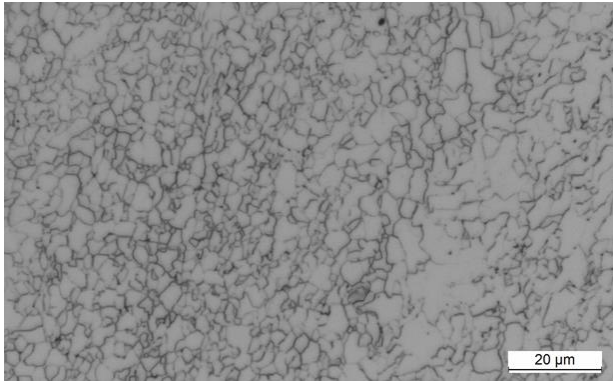


Figure 9. Room temperature microstructure (1420°C-1040°C condition).

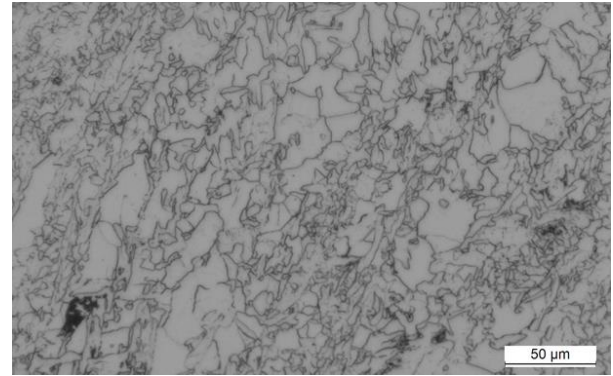


Figure 10. Room temperature microstructure (1420°C-1150°C condition).

3.3 Precipitation analysis

TEM analysis of quenched samples (before transformation) provided the following information:

- In the case of 1100°C equalization step and $T_1 = 1040^\circ\text{C}$, some Nb(C,N) precipitates with mean sizes between 20-50 nm were identified (Figure 11). These particles probably precipitated during the equalization step. In addition, some smaller particles were also observed. Taking into account their size, these particles could correspond to strain induced precipitates.
- When the equalizing temperature was increased to 1175°C and $T_1 = 1150^\circ\text{C}$, some particles of 20-50 nm were identified, but less abundant than in the previous case. In addition, the presence of possible strain induced particles was scarce.

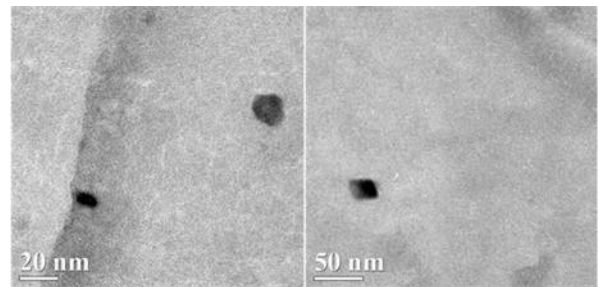
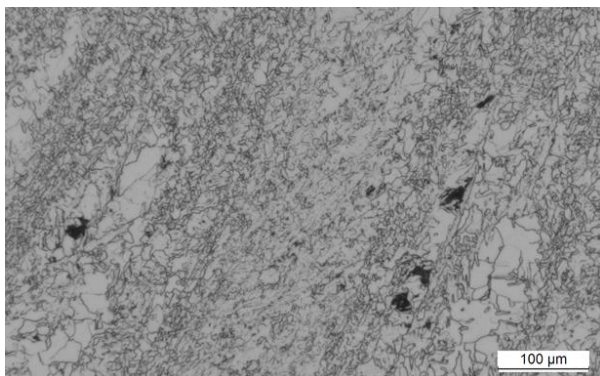


Figure 11. Particles in the range of 20-50 nm observed in quenched sample (1420°C-1040°C condition).

In relation to the room temperature microstructures, it was possible to identify a numerous population of very fine particles, as shown in the examples of Figure 12. This population was not present in the quenched conditions.

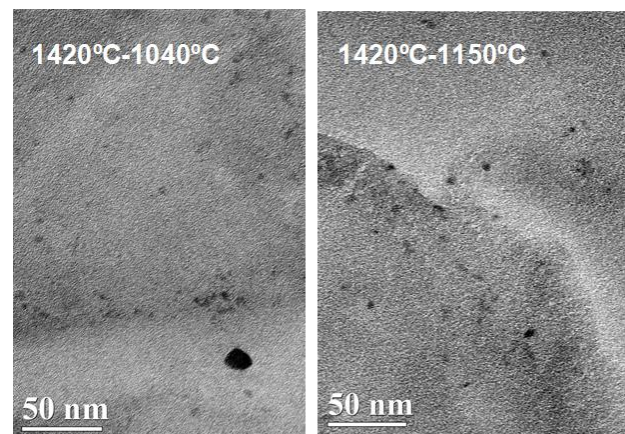


Figure 12. Fine Nb(C,N) precipitates in room temperature microstructures

Foil analysis of these room temperature microstructures confirmed that there was a fine Nb(C,N) precipitation, in some cases randomly distributed in the matrix and in

other associated with dislocations. Several examples are illustrated in Figure 13.

4 DISCUSSION

The four conditions analyzed provide different situations, although in all the cases a similar total reduction has been applied. The micrographs described in Figure 2 to Figure 8 denote that the initial austenite grain size and the rolling temperature schedule affect the conditioning of the austenite.

With the help of MicroSim model, it is possible to analyze the evolution of the austenite microstructure during deformation passes. The results corresponding to the evolution of the recrystallized fraction per pass are described in Figure 14. In this calculation, it has considered that not all the nominal Nb is in solution, based on previous studies that analyzed the effect of time in the equalizing step prior to deformation [7].

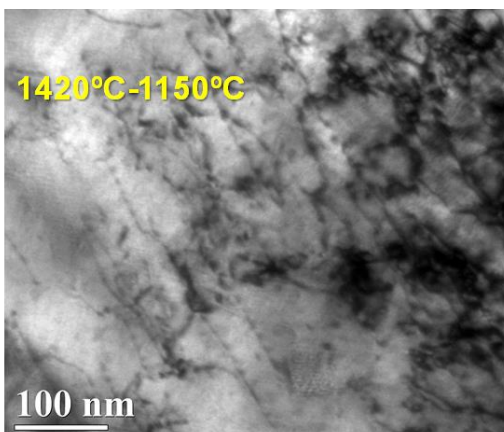
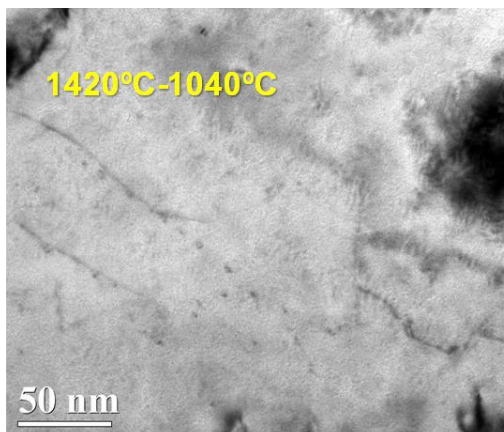


Figure 13. Nb(C,N) fine precipitates present in the ferritic microstructures.

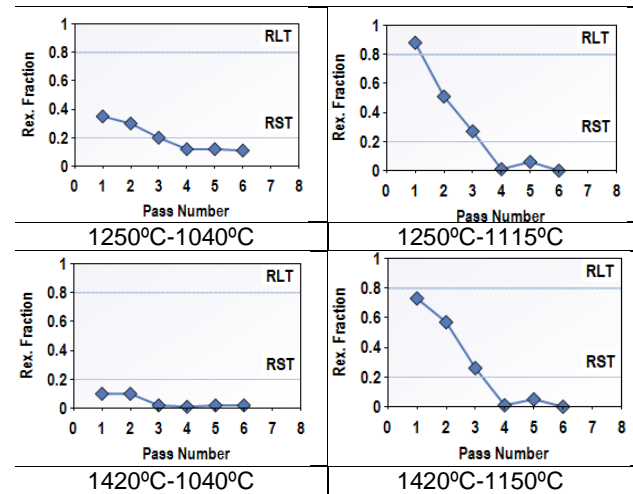


Figure 14. Evolution of the recrystallized fraction per pass predicted by MicroSim®.

In the figure, it is possible to observe some main differences depending on the low (1040°C) or high (1115-1150°C) initial deformation temperatures. In the $T_1 = 1040^\circ\text{C}$ conditions, the amount of recrystallized fraction remains low during all deformation sequences. This is significantly relevant in direct charging simulation with coarse initial austenite grains. In this case, the recrystallized fraction predicted by the model does not achieve the 20% of volume fraction in any case.

As the initial austenite grain size distribution exerts a relevant role in the microstructural evolution during deformation, in the following, a specific analysis of each case will be done.

4.1 Reheating conditions at 1250°C

In addition to the results shown in Figure 14, MicroSim model provides also other main data that are summarized as follows:

- For $T_1 = 1040^\circ\text{C}$, the recrystallized fraction occurring during all the passes is a mix of static and metadynamic. For $T_1 = 1115^\circ\text{C}$, metadynamic (combined with static) is only relevant in the initial passes. This agrees, at least qualitatively, with the characteristics observed in Figure 2 and Figure 3.

- In both cases, after pass 3, there is strain induced precipitation, but more relevant in $T_1 = 1115^\circ\text{C}$ condition.

Table 3 summarizes the characteristics of the austenite microstructure prior to transformation predicted by the model. In the table, the non-recrystallized fraction is divided depending if it is due to Nb(C,N) precipitation or to solute drag effect.

Table 3. Main austenite parameters prior to transformation predicted by MicroSim (1250°C)

T_1 (°C)	Rex (%)	No rex (%)		Acc. strain
		prec	drag	
1040	11	56	33	1.37
1115	0	94	6	1.42

The model predicts that, although the accumulated strain in austenite is quite similar in both cases, while for $T_1 = 1115^\circ\text{C}$ it is due to strain induced precipitation, for $T_1 = 1040^\circ\text{C}$ solute drag plays an important role.

Finally, looking the heterogeneity level of the quenched microstructures of Figure 2 and Figure 3 no clear conclusions can be obtained about each strategy. The differences are not conclusive as, after transformation, in both cases some heterogeneity level in ferrite grain sizes is observed (Figure 4 and Figure 5). On the other hand, the main aspect to consider is that the rolling strategy, identified this as the evolution of recrystallization and pancaking has been completely different. This also can be observed in the evolution of the accumulated strain per pass predicted by MicroSim and drawn in Figure 15, together with the recrystallized fraction (previously shown in Figure 14).

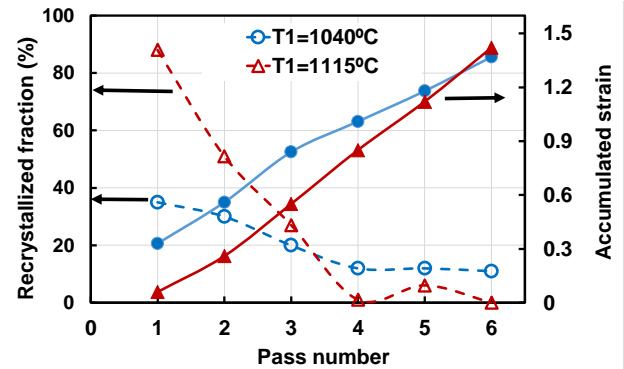


Figure 15. Evolution of recrystallized fraction and accumulated strain per pass predicted by MicroSim (1250°C).

4.2 Reheating conditions at 1420°C

The classical approach in TSDR is to develop a complete recrystallized microstructure in the initial passes, known as Type I regime, followed by a complete pancaked microstructure prior to transformation (Type II), as shown in the scheme of Figure 16. Usually, the mix condition of recrystallized and non-recrystallized microstructure (Type III) is considered as a transient situation that should be avoided as a final condition prior to transformation [8]. By applying this strategy, an homogeneous transformed room temperature microstructure should be obtained.

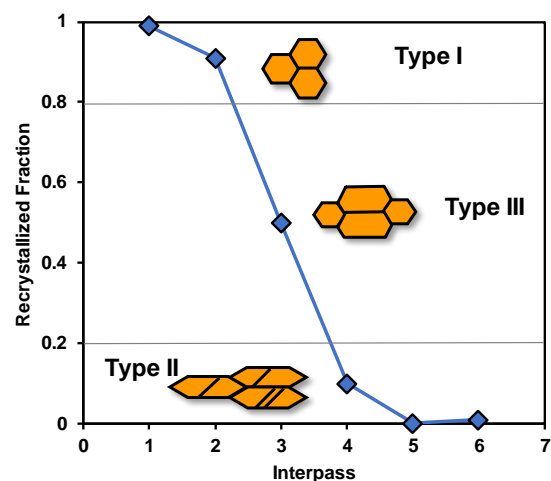


Figure 16. Scheme of "ideal" recrystallized austenite evolution per pass.

The results described in Figure 14 for $T_1 = 1040^\circ\text{C}$ denote a completely different

situation in relation to the scheme of Figure 16, while for $T_1=1150^\circ\text{C}$ the predictions are closer to the “ideal” case, although a high recrystallization fraction has not been achieved in the initial steps.

The predictions of MicroSim indicate that, in the case of $T_1=1040^\circ\text{C}$, the coarse as-cast grains combined with low initial temperatures do not favor the activation of dynamic recrystallization. In addition, as strain accumulates from pass to pass, strain induced precipitation occurs before any relevant recrystallization. These predictions, suggesting a very big pancaked microstructure, agree with the observations of Figure 6. The model predicts a total strain accumulation in austenite of 2.2 before transformation, significantly higher than those observed with the reheating at 1250°C tests.

In the case of $T_1=1150^\circ\text{C}$, MicroSim predicts the occurrence of some dynamic and metadynamic recrystallizations, in addition to the classical static one, due to the higher initial deformation temperatures (confirmed in Figure 7 and Figure 8). This leads to lower strain accumulation in initial passes, delaying the strain induced precipitation to interpass 3. In this case, the model predicts a total strain accumulation before transformation of 1.44. The comparison of the evolution of both, recrystallization fraction and accumulated strain are illustrated in Figure 17. As happened previously with the 1250°C reheating case, the resulting strategy in both cases is very different.

(1420°C).

The room temperature microstructure depends, in addition to other factors, on the austenite conditioning. In both cases, Figure 9 and Figure 10, it is possible to identify very fine ferrite grains (in the range of 3-4 μm), but in contrast to what it could be expected, the fraction of heterogeneous areas with coarse ferrite grains, was lower in the $T_1=1040^\circ\text{C}$ condition. Nevertheless, these fractions remained very high.

In order to evaluate if a higher total reduction could enhance dynamic recrystallization activation, a new multipass torsion simulation was performed, in this case, with a total reduction pass that could correspond to a final sheet thickness of 4 mm. The resulting microstructures are shown in Figure 18 for the case of $T_1=1040^\circ\text{C}$. The quenched austenite microstructure confirms that, as the model predicted, the low initial temperatures did not favor the activation of dynamic recrystallization as strain induced precipitation took place immediately after second interpass time. The higher total reduction applied in this case had two beneficial effects: an increase of static recrystallization fraction in initial passes and a higher final strain accumulation. Both factors, once transformed the microstructure during cooling down, decreased in one third the amount of heterogeneous regions. Nevertheless, they remain relevant, as can be observed in Figure 18.

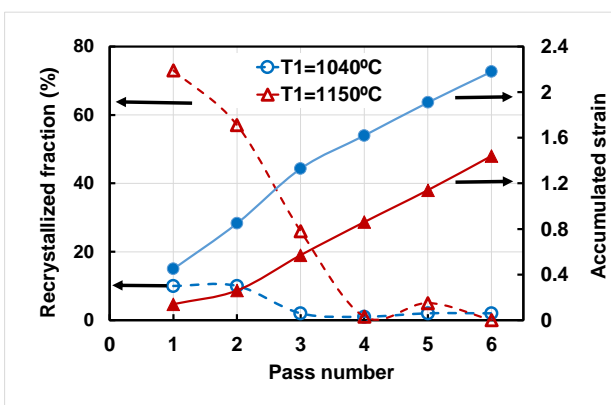


Figure 17. Evolution of recrystallized fraction and accumulated strain per pass predicted by MicroSim



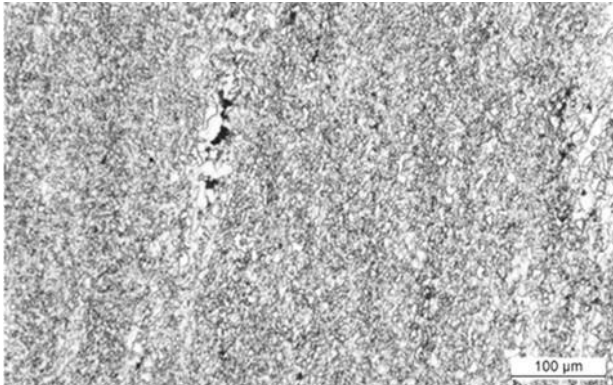


Figure 18. Microstructures after quenching and at room temperature (1420°C-1040°C condition and simulated final thickness of 4 mm).

The microstructural analysis of the quenched samples denote two different problems that are affecting the heterogeneity appearance in room temperature microstructures. In the case of high pancaked situations, as those obtained with $T_1 = 1040^\circ\text{C}$, it is possible to observe important differences in the amount of internal defects present in the elongated austenite grains, as shown in the example of Figure 6. These internal defects will enhance intragranular nucleation of ferrite grains, promoting the very fine microstructure observed in the homogeneous regions (see Figure 19). In contrast, the aspect of the ferrite grains in the heterogeneous regions, see Figure 20, suggest the lack of intragranular nucleation during transformation and the growth of ferrite grains nucleated at grain boundaries until their impingement.

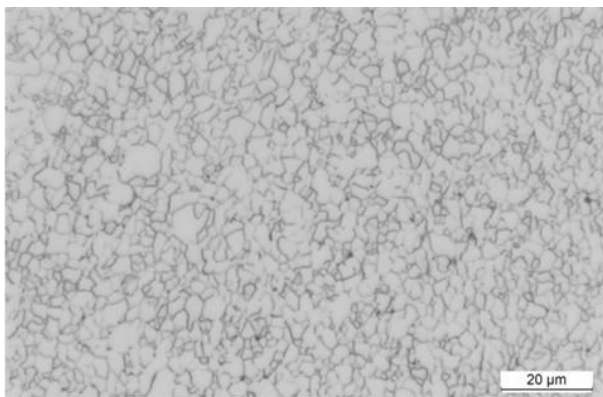


Figure 19. Homogeneous ferritic region (1420°C-1040°C condition).

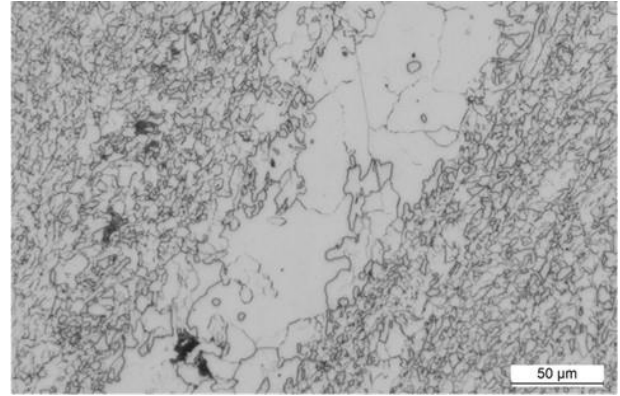


Figure 20. Heterogeneous region suggesting lack of intragranular nucleation in austenite defects (1420°C-1040°C condition).

The results shown in Figure 18, with a higher total reduction applied leading to a higher accumulated strain, suggest that, by doing this, the problem of the lack of intragranular nucleation sites in pancaked austenite can be partially reduced, but it is not sufficient to achieve a complete homogeneous microstructure.

The second problem to consider is illustrated in Figure 8. The activation of softening mechanisms, including different recrystallization types, is characterized by an important local heterogeneity. This combined with the different density of internal defects in remaining non-recrystallized grains, lead to the heterogeneities that are present in the final microstructure.

Both aspects are probably related to the different crystallographic orientations of some austenite grains in relation to the rest of microstructure, but this remains an open question.

Finally, the analysis of the laboratory simulations has shown different aspects of how Nb interacts during austenite evolution. For example, its role as solute drag factor delaying static recrystallization is a key tool in conditions as those happening in the 1250°C-1040°C simulation, while strain induced precipitation appears as the main tool in the other cases.

On the other hand, in addition to the final room temperature grain refinement, that both solute drag and strain induced

precipitation help to achieve, Figure 13 shows the other mechanism, precipitation hardening, that needs to be considered. The balance between “*solute drag*”, “*strain induced precipitation*” and “*precipitation hardening*”, that can be obtained with Nb, will depend on a proper design of the thermomechanical processing parameters. And in addition to the usually accepted variables (reduction per pass, interpass time, temperature...), the nature of the austenite microstructure, including the amount of Nb in solution and precipitated at the entry of the first rolling pass, is another key factor in these complex interactions.

4 CONCLUSIONS

This study has been focused on the different interactions that can happen during hot working between softening mechanisms, strain induced precipitation and strain accumulation and how, they can affect the final room temperature microstructural homogeneity in Nb microalloyed grades.

Different extreme scenarios have been evaluated and they show that:

- Initial austenite microstructure, including grain size distribution and amount of Nb precipitated and in solution, affects the evolution of the microstructure during hot rolling.
- As initial austenite grain size becomes coarser, more attention must be paid to the heterogeneous nature of recrystallization nucleation and austenite intragranular defect density.
- These two characteristics need to be considered to define proper rolling strategies when high mechanical properties, requiring a high degree of microstructural homogeneity, become mandatory.

Acknowledgments

The authors would like to gratefully acknowledge Companhia Brasileira de Metalurgia e Mineração (CBMM) for funding this study.

REFERENCES

- 1 N. Isasti, B. López, J.M. Rodriguez-Ibabe, L. Martínez and A.K. Hatui. Development of ferritic-bainitic Nb microalloyed steels by CSP route. Inter. symp. on thin slab casting and direct rolling (TSCR); 2018; 80-87.
- 2 B. Linzer, A. Jungbauer, G. Wersching, A. Viehböck, Y. Changjiang, Y. Yao, and Q. Linlei. The new world of hot strip rolling – Achievements at Rizhao steels’s new ESP complex setting new standards. BHM. 2016; 161(9): 421-428.
- 3 P. Uranga, B. Lopez and J.M. Rodriguez-Ibabe. Role of carbon and nitrogen content on microstructural homogeneity in thin slab direct rolled microalloyed steels. Ironmaking Steelmaking. 2009; 36(3): 162-169.
- 4 B. Pereda, B. Lopez and J.M. Rodriguez-Ibabe. Relevance of static and dynamic recrystallizations on austenite grain refinement in Nb-Mo microalloyed steels. Thermec 2009. Mater Sci Forum. 2010; 638-642: 3350-3355.
- 5 MicroSim-DSP® Software. Ceit (San Sebastian, Spain). 2018; v9.
- 6 J.M. Rodriguez-Ibabe. Thin slab direct rolling of microalloyed steels. Mater Sci Forum. 2005; 500-501: 131-138.
- 7 G. Larzabal, L. Garcia-Sesma, B. Pereda, P. Uranga, M. Rebellato, B. López and J.M. Rodriguez-Ibabe. Validation of an indirect technique to quantify the amount of Nb in solution prior to hot rolling. MST 2016; 509-516.
- 8 J.M. Rodriguez-Ibabe, P. Uranga and B. Lopez. Some aspects regarding microstructural heterogeneities during steel processing. Thermec 2011. Mater Sci Forum. 2012; 706-709: 157-164.